MSFC-103

An Evaluation of Grazing-Incidence Optics for Neutron Imaging

M.V. Gubarev[a], B. D. Ramsey[b], D. E. Engelhaupt[c], J. Burgess[c], D.F.R. Mildner[d]
a) Universities Space Research Association, MSFC/NASA, VP62, Huntsville, AL 35812
b) Marshall Space Flight Center /NASA, Huntsville, AL 35812
c) Center for Applied Optics, University of Alabama in Huntsville, AL 35899
d) Center for Neutron Research, National Institute of Standards and Technology, Gaithersburg, MD 20899

Abstract

The focusing capabilities of neutron imaging optics based on the Wolter-1 geometry have been successfully demonstrated with a beam of long wavelength neutrons with low angular divergence.. A test mirror was fabricated using an electroformed nickel replication process at Marshall Space Flight Center. The neutron current density gain at the focal spot of the mirror is found to be at least 8 for neutron wavelengths in the range from 6 to 20 Å. Possible applications of the optics are briefly discussed.

1. Introduction

The optical properties of materials are characterized by their refractive indices. In the case of thermal neutrons, the refractive index is slightly less than unity by about 10^{-5} for most elements and their isotopes[1]. Consequently, thermal and cold neutrons can be reflected from smooth surfaces at shallow 'grazing-incidence' angles (total external reflection) or be refracted at boundaries of different materials.

Optical elements for neutrons can be designed to simply concentrate the neutron current or to produce a true image of the neutron source. An example of former is polycapillary optics in which neutrons undergo multiple reflections from capillary walls to emerge in a new direction[2]. Arrays of capillaries, with a common focus, can converge a quasi-parallel beam of neutrons to increase the current density [3]. Alternatively, concave refractive lenses[4]can be used both for neutron flux enhancement and for true imaging. However, the refractive index depends on the square of the neutron wavelength so that refractive optics are strongly chromatic and high performance can only be achieved with monochromatic neutron beams.

Optics based on total external reflection are achromatic, but to date these have been limited to toroidal single-bounce mirror systems[5] with higher aberrations than refractive lenses. However, reflective optics based on the so-called Wolter geometries[6] that are used extensively in x-ray astronomy can also be designed for use with neutron beams. The optical scheme most widely used is a Wolter-1 geometry whereby two consecutive reflections from parabolic and hyperbolic surfaces are used to focus the x-rays, as shown in Figure 1. The mirrors have a cylindrical form, so that optics with different diameters, but the same focal length, can be nested together to increase the system throughput.

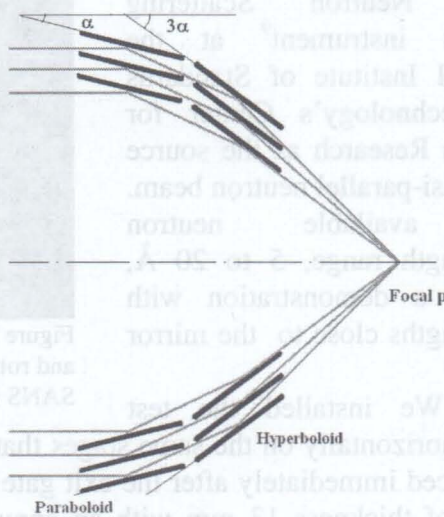

Figure 1: Optical system based on the Wolter-1 geometry. Parabolic and hyperbolic surfaces are oriented at angles α and 3α to the incident radiation. This configuration gives coma-free imaging off axis.

The primary aim of the research presented here was to demonstrate the feasibility of neutron imaging using the double-reflection grazing-incidence geometry. We present performance results of preliminary tests of a neutron mirror, based on the Wolter-1 geometry, fabricated at NASA's Marshall Space Flight Center (MSFC).

2. Optics testing results and discussion

The technique that we have used to produce the test mirror is the electroformed nickel replication (ENR) process, which we have been developing at MSFC for hard-x-ray astronomy[7]. In this technique, pure nickel or nickel-alloy mirror shells are electroformed onto a figured and superpolished nickel-plated aluminum cylindrical mandrel from which they are later released by differential thermal contraction. The resulting cylindrical mirror has a monolithic structure that contains both the parabolic and hyperbolic segments.

We have utilized an existing 62-mm diameter, 175-mm long, 1-m focal length mandrel originally designed as a 1/10-scale version of the innermost mirror of NASA's Chandra X-Ray Observatory[8]. This optic has appropriate graze angles (α = 8.0 mrad) for cold neutron reflection. The critical angle for total external reflection of neutrons is 1.73 mrad $Å^{-1}$ for a natural nickel surface, so that the cut-off wavelength for this optic is 4.6 Å. From measurements of the mirror mandrel we estimated that the microroughness of the final mirror surface was less than 5 Å rms.

An evaluation of the x-ray performance of the mirror was carried out at the Stray Light Facility at MSFC. The optic was placed 100 meters from a 0.2-mm-diameter x-ray source, mounted on tip-tilt stages to aid alignment, and with a pinhole-collimated x-ray detector located at the focal position. The half power diameter of the mirror for an energy range from 6 to 8 keV, calculated from flux measurements within different pinhole diameters, was found to be 0.140 ± 0.003 mrad, which corresponds to a focal spot size of about 140 micron diameter. We expect a comparable focal spot size for a neutron beam, but only if the beam has a divergence similar to the micro-radian level divergence of the test x-ray beam.

We evaluated the neutron performance of the test optic using the NG-7 Small-Angle Neutron Scattering (SANS) instrument[9] at the National Institute of Standards and Technology's Center for Neutron Research as the source of a quasi-parallel neutron beam. The available neutron wavelength range, 5 to 20 Å, permits a demonstration with wavelengths close to the mirror cut off.

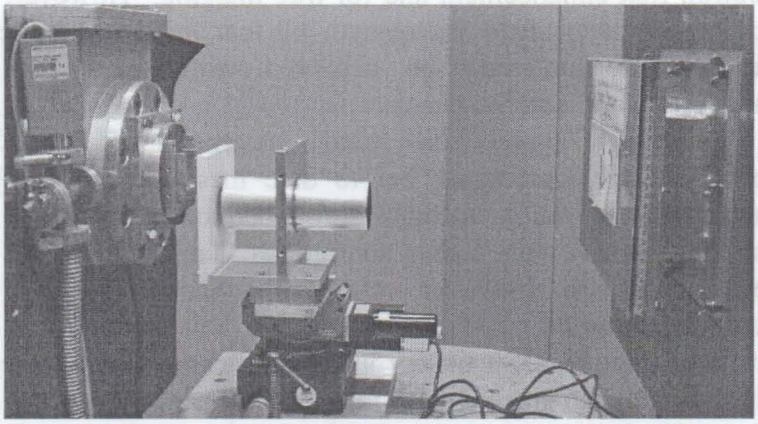

Figure 2: The test mirror installed in the neutron beamline on tip-tilt and rotation stages. At left is the beam exit gate. At right is the NG-7 SANS instrument sample box attached to the detector system.

We installed the test mirror horizontally on the same stages that were used for the x-ray evaluation and the assembly was placed immediately after the exit gate of the beamline (Figure 2). A plate made from boron nitride of thickness 13 mm with an annular aperture was placed between the mirror and the beamline exit window. The aperture extent was slightly larger than the maximum beam diameter of 25 mm available at NG-7. Because of this finite beam size, the beam was only illuminating

the top portion of the mirror, corresponding to a geometric area of approximately 18 mm^2. The beamline detector was a He^3 position-sensitive proportional counter with 128 x 128 pixels, each 5 mm by 5 mm in area, positioned at a controllable distance from the test optic.

A direct measurement of the focal spot size of the mirror is not possible because the spatial resolution of the SANS detector is much poorer than the expected focal spot size. Moreover, the configuration of the instrument sample area is such that the closest distance between the optic and the detector is slightly greater than the mirror focal distance of 1 meter.

The mirror focal spot size can, however, be estimated from measurements of the extra-focal mirror annulus width. The neutron beam reflected from the optic forms a "shrinking" semicircular annulus which projects to a nominal point at the mirror focus and then expands again beyond this. A series of measurements at various detector-to-focal spot distances can demonstrate this focusing (or in this case de-focusing) action of the neutron mirrors. With the mirror installed immediately after the beamline exit gate, the detector can be positioned at any distance between 1.65 m and 17.65 m from the center of the mirror.

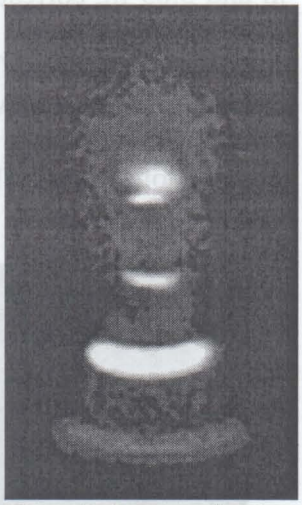

Figure 3. An extra-focal image taken at 4.67 meter behind the focal point of the mirror using the 10 Å. neutron

The Wolter-1 geometry calls for the tilt angle of the hyperbolic section to be three times larger than the tilt angle of the parabolic section of the mirror to preserve the graze angle throughout (see Figure 1). Having two mirror sections means that in some circumstances there can be up to three components to the reflected beam: 1) the expected double bounce component where neutrons reflect from the parabolic then the hyperbolic sections; 2) a single bounce component where neutrons reflect from the parabolic stage only; and 3) a single component from the hyperbolic stage only. Component (2) arises in cases where the incoming beam is divergent or off axis. In this case the increase in graze angle from the first section means that some neutrons miss the second section altogether. Component (3) is always present if the critical angle for the neutron beam is greater than the grazing angle of the hyperbolic section. In a nested system of mirrors, however, this component is greatly suppressed by self shielding. Naturally, beam component (3) comes to a focus before the true (component (1)) focus position, and so does not contaminate the image.

For neutron optics evaluation tests, the mirror was aligned with the NG-7 quasi-parallel beam using 10 Å neutrons and all the instrument neutron guides installed. The critical angle of the guide's nickel surface is 17.3 mrad for 10 Å neutrons and this determines the divergence of the neutron beam. This divergence is much larger than the graze/tilt angle of the parabolic section of the mirror. Under these circumstances, the detector image shows four components from the irradiated optic (Figure 3). The almost circular image with a small annulus below at the top of the figure represents the portion of the incoming beam that passes through the annular slit but above and below the mirror and thus is not reflected. The next three annular features, growing in extent, represent components (2), (1) and (3) discussed above, respectively, moving from top to bottom of the figure. Component (3) is very faint because the hyperbolic section tilt angle is larger than the critical angle for the mirror's nickel surface at 10 Å neutron wavelength, and thus only a tiny portion of the neutron beam can be reflected. The mirror and the neutron beam were aligned so their axes were parallel. In this case the three images that represent the single and double reflected beams are coaxial and equidistant as is seen in Figure 3.

We have investigated the performance of the mirror with measurements made at neutron wavelengths of 6 Å, 10 Å and 20 Å, each with a bandwidth of about 11%. All the instrument's neutron guides were removed to obtain the lowest possible beam divergence, with the size of the first aperture of the collimation reduced to 14 mm, while the exit aperture remained at 25 mm in diameter. The optic was located about 15 meters from the 14 mm aperture, so that the neutron beam divergence for this configuration was estimated to be less than 1 mrad. Semicircular annulus images were collected for each wavelength at optic-to-detector distances of 1.65 m, 3,65 m and 5.65 m, corresponding to detector-to-mirror focal spot distances of 0.67 m , 2.67 m and 4.67 m respectively. Figure 4 shows an example of the annulus images taken for 20 Å wavelength neutrons. The image of the beam at the top of the figure represents the portion of the incoming beam that was not reflected. Below this are components (1) and (3) respectively. Component (2) is not now seen as the divergence of the beam has been reduced considerably. The area of the optic illuminated by the neutron beam was calculated by triangulation to be 17.7 mm^2.

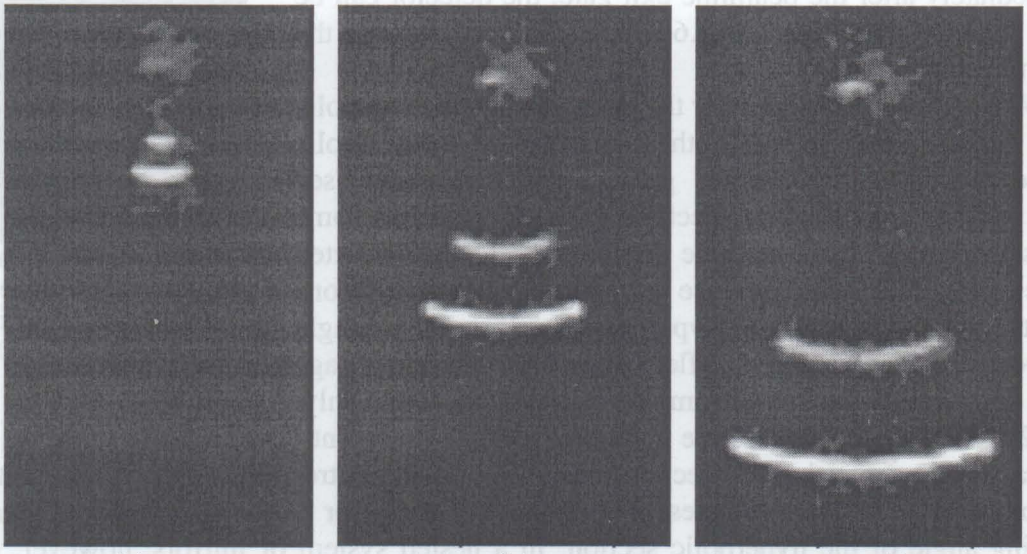

(a) (b) (c)

Figure 4. The mirror extra-focal annulus images taken for 20 A wavelength neutrons at (a) 0.67 m, (b) 2.67 m and (c) 4.67 m from the mirror focal spot.

We have estimated the double-bounce-annulus (component (1)) width from the images taken at the 5.65 m detector-to-optic distance position. The total length of the annulus image was found to be 23 pixels using summed multiple pixels to improve statistics. To estimate the FWHM of the radial annulus size, a measure of the angular resolution of the optic, a Gaussian curve was fit to the profile of the annulus. The angular size of the annulus was found to be ~ 1.15 mrad for all three wavelengths. At the focal distance of 1 meter, this angular size corresponds to a focal-spot size (FWHM) of about 1.15 mm, about a factor of eight greater than that derived from the x-ray test data. Note, however, that the dominant factor here is the divergence of the incident beam which we estimate to be at about the 1 milliradian level, close to the measured resolution of the optic.

To measure the neutron flux in the incident beam, the optic was replaced with a 6.4-mm diameter pinhole made in a boron nitride plate, and the straight-through rate measured in the

detector. The resulting incident beam intensity is then used to calculate the effective area of the mirror, i.e. the incoming beam cross-sectional area that would contain the same number of neutrons as in the mirror double-bounce annular image. We calculated the gain in neutron current density achieved by virtue of the focusing action of the mirror assuming the mirror focal spot size is 1.15 mm (FWHM). Table 1 shows the results of these calculations. The effective-area measurements are in good agreement with the calculated area of 17.7 mm^2, indicating that the neutron beam was focused without loss. The gain in neutron current density at the mirror focal spot is estimated to be ~ 8 for all three wavelengths. With the wall thickness of the mirror about 1 mm, the footprint area of the optic at the beam is only 44 mm^2. The use of nested mirrors can improve the neutron current density gain by approximately an order of magnitude, even in the case of this 25-mm-diameter divergent beam.

Table 1. The effective area and gain measured for the test mirror

Neutron wavelength, Å	Effective area, mm^2	Gain
6	17.9±0.4	8.5
10	17.1±0.2	8.2
20	15.8±1.6	7.6

3. Conclusion

These experiments have successfully demonstrated the feasibility of grazing-incidence neutron optics. This opens the possibility of developing imaging systems for either finite or infinitesource-distance applications using Wolter geometries. The ENR technology has been shown to be capable of producing x-ray optics with angular resolutions as high as 10 arc seconds (~ 50 μrad)[10]. Thus, we should expect neutron optics with similar angular resolutions. The ability of neutrons to penetrate heavy materials but be attenuated by some light elements enables such neutron imaging to complement other techniques. Biological microscopy and neutron radiography can also benefit from high resolution neutron optics.

The presence of water on the planets can also be inferred from neutron measurements. Produced at high energies in the lunar or Martian regolith by the action of cosmic rays, neutrons are slowed down to low or 'thermal' energies through collisions with light elements, such as the hydrogen in water. A large increase in thermal neutrons, and a corresponding decrease in epithermal ones, measured for example from orbit, indicates the possibility of substantial water deposits. The lunar prospector mission using crudely collimated neutron detectors with ~ 100 km surface resolution, has found a substantial increase in thermal neutrons at the lunar poles[11]. The use of neutron optics will substantially increase the signal to noise ratio and also improve the spatial accuracy for these neutron mapping measurements.

Grazing incidence optics can also be used to focus neutrons in SANS experiments. Here, the beam penumbra can be significantly decreased by arranging for the focus to be at the detector, resulting in lower values of obtainable scattering angles. The high efficiency of the optics permits a decrease in the minimum scattering vector without lowering the neutron intensity on sample. In this application, a significant advantage of the reflective optics over refractive optics is that the focus is independent of wavelength, so that the technique can be applied to polychromatic beams at pulsed neutron sources using time-of-flight.

Finally, we note that ENR-fabricated mirrors can be used as substrates for multilayer coatings[12]. The use of these will significantly extend the neutron wavelength range of the grazing incidence optics, possibly into the epithermal region.

Acknowledgements

We gratefully acknowledge: the support of the National Institute of Standards and Technology, U.S. Department of Commerce, in providing the neutron research facilities used in this work; Jeff Krzywon for his help at NG-7; John Barker for his useful comments and discussion.

This work was supported in part by NASA through MSFC Individual Research and Development Program and Cooperative Agreement NCC8-259.

References

[1] "Neutron Optics", V.F. Sears, Oxford University Press, (1989) 64.

[2] D. F. R. Mildner, H. H. Chen-Mayer, W. M. Gibson, and A. J. Schultz, Proc. SPIE 4785 (2002) 43.

[3] H.Chen, R.G Downing, D.F.R. Mildner, W.M. Gibson, M.A.Kumakhov, I.Yu. Ponomarev and M.V. Gubarev, Nature,v. 357, (1992) 391.

[4] J.T. Cremer, M.A. Piestrup, C.K. Gary, R.H. Pantell, C.J. Glinka, Appl Phys Letters 85 (2004) 494.

[5] C. Hayes, C. Lartigue, A. Kollmar, J.R.D. Copley, B. Alefeld, F. Mezei, D. Richter and T. Springer, J. Phys Soc Jpn Suppl. A 65 (1996) 312.

[6] H. Wolter, Annalen der Physik 445 (1952) 28.

[7] B. D. Ramsey, R F. Elsner, D. E. Engelhaupt, M. Gubarev, J. J. Kolodziejczak, S. L. O'Dell, C. O. Speegle and M. C. Weisskopf, Proc. SPIE v. 5168, (2003) 129.

[8] http://cxc.harvard.edu/cdo/about_chandra/overview_cxo.html

[9] C.J. Glinka, J.G. Baker, B. Hammouda, S. Krueger, J.J. Moyer and W. J. Orst, J. Appl Cryst 31 (1998) 430.

[10] "M. Gubarev, C. Alexander, B. Ramsey, Proc. SPIE 5900 (2005) 232.

[11] http://nssdc.gsfc.nasa.gov/planetary/lunarprosp.html

[12] Romaine, S.; Basso, S.; Bruni, R. J.; Burkert, W.; Citterio, O.; Conti, G.; Engelhaupt, D.; Freyberg, M. J.; Ghigo, M.; Gorenstein, P.; Gubarev, M.; Hartner, G.; Mazzoleni, F.; O'Dell, S.; Pareschi, G.; Ramsey, B. D.; Speegle, C.; Spiga, D. Proc. SPIE 6266 (2006) 1C1.